Deep trap states in rubrene single crystals induced by ion radiation

Tino Zimmerling,[1,*] Kurt Mattenberger,[1] Max Döbeli,[2] Marius Johannes Simon,[2] and Bertram Batlogg[1]
[1]*Laboratory for Solid State Physics, ETH Zurich, 8093 Zurich, Switzerland*
[2]*Ion Beam Physics, ETH Zurich, 8093 Zurich, Switzerland*

(Received 29 November 2011; revised manuscript received 4 January 2012; published 4 April 2012)

Rubrene single crystals have been irradiated with 1-MeV protons and helium ions at various fluence levels (0.1×10^{12}–5×10^{12} particles/cm^2), and the resulting increase of the density of bulk trap states (DOS) has been studied by temperature-dependent space-charge-limited current measurements. Irradiation creates a peak in the trap DOS (about 10^{16} traps/cm^3 for a radiation dose of ≈35 J/g), centered at ≈0.35 eV above the valence band edge. With incrementally increasing radiation dose, the induced trap density rises sublinearly and saturates at high dose. Three to five times more traps are created if the crystal surface is not covered during irradiation. We attribute this trap creation primarily to C–H bond breaking accompanied by hydrogen loss.

DOI: 10.1103/PhysRevB.85.134101 PACS number(s): 81.05.Fb, 61.82.Pv, 61.72.−y

I. INTRODUCTION

Over the past two decades there has been impressive progress in the performance of electronic devices based on organic semiconductors, moving them from the realm of universities to industrial R&D, and even to first low-cost consumer products such as light-emitting diodes.[1] Improved fabrication methods and novel materials have been the driving force behind this development.[2] However, the performance of the devices is limited by a high density of imperfections which cause charge carriers to be trapped.[3,4] Developing a deeper understanding of the various ways such traps are created is a central challenge to be addressed in detailed studies.

Trap states are known to arise mainly from growth-related structural disorder, chemical impurity, and nonperfect interfaces. After device fabrication, traps may arise due to thermal stress, causing the formation of grain boundaries[5] or x-ray irradiation observable in a shift of the threshold voltage in a field-effect transistor.[6] For a more detailed and fundamental understanding of defect-related trap states, it is highly desirable to study both the density of traps and their energy position in response to a deliberate perturbation of the semiconductor. Single crystals excel an intrinsically low trap density of states (DOS)[3] and are thus well suited to study trap formation in a controlled way.

We have induced defects in rubrene crystals by proton and He^+ irradiation and have quantified them by temperature-dependent space-charge-limited current (TD-SCLC) measurements. The resulting electronic trap levels are found to be located at around 0.35 eV above the valence band (VB) edge. With incrementally increasing radiation dose, the trap density initially grows sublinearly and eventually levels off.

II. EXPERIMENT

The sample fabrication starts with the growth of rubrene single crystals by physical vapor transport in a controlled flow of argon.[7] Thin crystals (∼1 μm) were electrostatically bonded against bottom chromium/gold electrodes evaporated through a shadow mask on a cleaned glass substrate. Two methods were used to apply the top electrode: either gold is evaporated onto the crystal or onto a flexible piece of polydimethylsiloxane (PDMS) with a chromium adhesion layer,[8] which is in turn placed on top of the crystal. The top electrode is oriented perpendicular to the bottom electrode, resulting in a sandwichlike structure, as illustrated in Fig. 1, with an electrode cross section of usually 45 μm × 45 μm. To derive the density of bulk trap states, we performed temperature-dependent current-voltage measurements through the crystal bulk and analyzed them in terms of TD-SCLCs.[8–11]

Defects in the crystals were introduced by irradiating them with 1-MeV protons or helium ions (He^+) at various controlled fluence levels, ranging from 0.1×10^{12}–5×10^{12} particles/cm^2, provided by a 6 MV tandem Van de Graaff accelerator. As a side remark, an equivalent fluence of 1-MeV protons is experienced by a satellite in geostationary orbit during one year.[12,13] An energy of 1 MeV is large enough for the ions to penetrate a typical 1-μm-thick crystal; hence, no ions remain in the crystal, and the damage is uniform in depth. To avoid channeling effects, the samples were tilted by 10° relative to the normal ion incidence. Samples were handled and mounted in ambient atmosphere. The crystals have been irradiated in the dark and in high-vacuum conditions (∼10^{-7} mbar) for some seconds up to several minutes, depending on the beam current and type of ion.

We have measured the trap density for several exposures to determine the stepwise change of the trap DOS with increasing dose. Therefore, the very same crystal had to be cooled down several times to 150 K for TD-SCLC measurements with intact contacts. To enhance the reliability of the experiment and to separate the irradiation effects from possible other influences, only one part of the crystal was irradiated while the other was shielded by a 80-μm-thick metal plate which gives a reference, as depicted in Fig. 1.

III. RESULTS AND DISCUSSION

The results for the density of states are based on five rubrene crystals and provide a consistent picture about the energetic position of the electronic trap states, the dose-response behavior, and thus the underlying mechanism of damage. First we discuss the impact of ion irradiation on the current-voltage characteristics and the resulting density of states.

 ©2012 American Physical Society

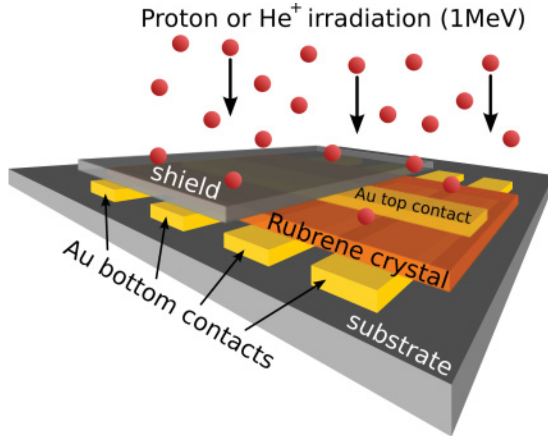

FIG. 1. (Color online) A rubrene crystal sandwiched between two gold contacts allows current-voltage measurements through the crystal bulk and the derivation of the density of bulk trap states. The crystal is partly shielded by a metal plate during irradiation to protect the crystal underneath that serves as reference.

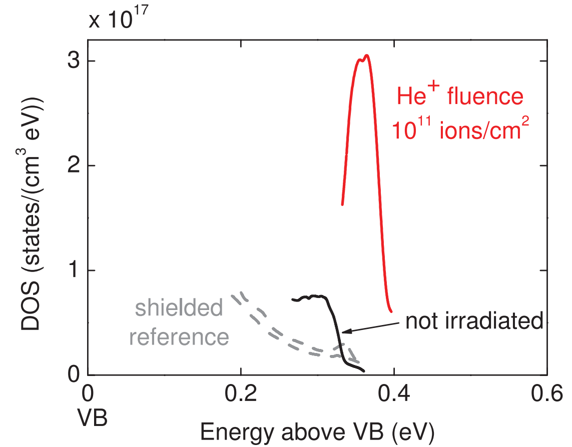

FIG. 3. (Color online) The density of states for the shielded (dashed) reference and the irradiated (solid) rubrene crystal (crystal 3) before and after exposure to 10^{11} He ions/cm^2. The irradiation caused the creation of a sharp trap peak at approximately 0.35 eV above the VB.

Figure 2 shows I-V curves measured at different temperatures of a shielded reference and an unshielded crystal before and after irradiation with He^+. (Only 3 out of 10 temperatures are shown for clarity.) The shielded reference exhibits only minor changes, whereas the onset of significant current flow of the irradiated crystal shifts to higher voltages. As discussed in an earlier publication,[9] the data analysis in terms of the trap DOS does not depend on such voltage shifts. Rather, the relevant energy scale of the trap DOS is related to the activation energy E_A, which is determined from the Arrhenius plot at a given measurement voltage V. The self-consistent analysis also considers the shift of E_A as a function of V and thus excludes the V range that is dominated by contacts.[9–11,14]

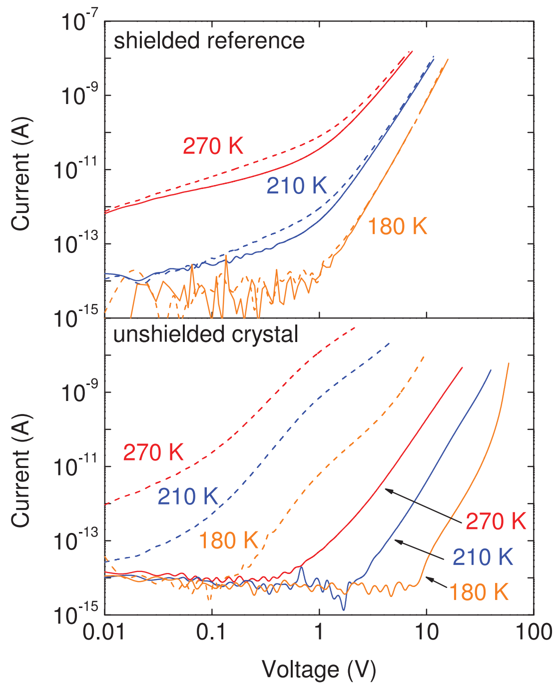

FIG. 2. (Color online) SCLC measurements of the shielded and unshielded crystal part before (dashed) and after (solid) the irradiation for selected temperatures. No significant changes are obtained for the shielded crystal. In contrast, the I-V curves of the unshielded crystal shift to higher voltages.

Based on the measurements presented in Fig. 2, we extracted the trap DOS as shown in Fig. 3. The DOS of the shielded reference remains unchanged within experimental uncertainty. However, a distinct trap peak is induced in the irradiated crystal.

Figure 4 shows the creation of a trap peak in a rubrene crystal irradiated three times with protons. (The trap density was measured within one day after each irradiation step.) Again, it is worth noting that the DOS of the shielded reference remains, indeed, unaffected within experimental uncertainty, despite multiple coolings, measurements, and sample transfers. In contrast, proton radiation of the unshielded part induces a pronounced trap peak that is about 0.2 eV wide and is centered at around 0.35 eV above the VB edge. The induced trap density is of the order 10^{16} cm^{-3} and thereby roughly 10^3-fold higher than the trap density induced in silicon with a similar dose.[15] Remarkably, the trap density grows sublinearly with increasing fluence (lower part of Fig. 4).

The impact of protons and He^+ can be compared by calculating the radiation dose D, defined as the energy deposited per unit mass of the target material. The stopping power dE/dx in rubrene (and in the top electrode) is determined using the SRIM code,[16] yielding the radiation dose

$$D = \frac{N \frac{dE}{dx} d}{m}, \tag{1}$$

where N is the number of ions penetrating the electrode cross-section area, d is the crystal thickness, and m is the mass of the crystal volume probed by current-voltage measurements. The uncertainty of the estimated dose is about ±10%.

In Fig. 5, the induced trap DOS of proton and He^+-irradiated samples is shown, each of them exposed to a dose of 35 J/g. The associated temperature rise of the crystal is estimated to be about 30 °C, assuming thermal isolation.

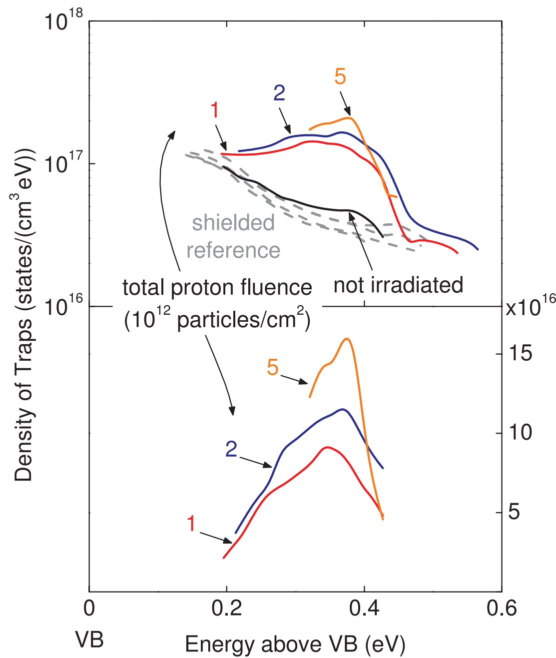

FIG. 4. (Color online) The density of trap states for three doses of irradiation with 1-MeV protons is shown for the shielded part (dashed lines) and irradiated part (solid lines) of crystal 1.4. In the upper figure, the DOS is given on a logarithmic scale. In the lower figure, the trap DOS of the nonirradiated crystal is subtracted from the trap DOS after each irradiation step and plotted on a linear scale. Trap states are introduced in a broad energy range with a peak at approximately 0.35 eV above the VB edge. With increasing fluence the density of induced traps grows sublinearly. (See also Fig. 6.)

All curves are consistent with the creation of a generic trap peak at around 0.35 eV above the valence band edge. In addition, the number of induced traps (integrated area below the curves) is of the order 1.8×10^{16} states/cm^3 (see also Fig. 6). However, one peak in Fig. 5 is sharper in energy, though with approximately the same area. We interpret this particular example as indication that ion irradiation creates an

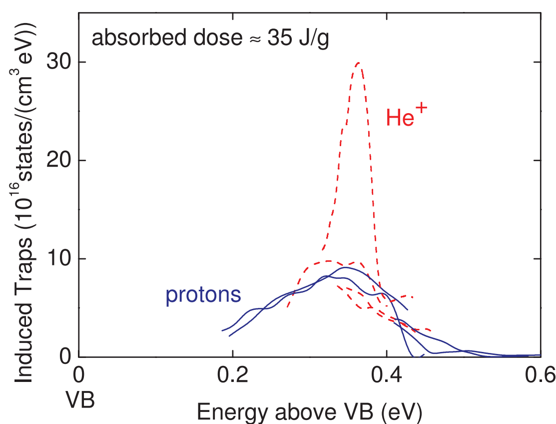

FIG. 5. (Color online) Radiation-induced trap DOS in five crystals that absorbed approximately 35 J/g from proton (solid) or He$^+$ (dashed) radiation. (Two of them had two intact irradiated contacts.) Trap peak position and density of traps created (see also Fig. 6) are consistent for the creation of a generic trap peak.

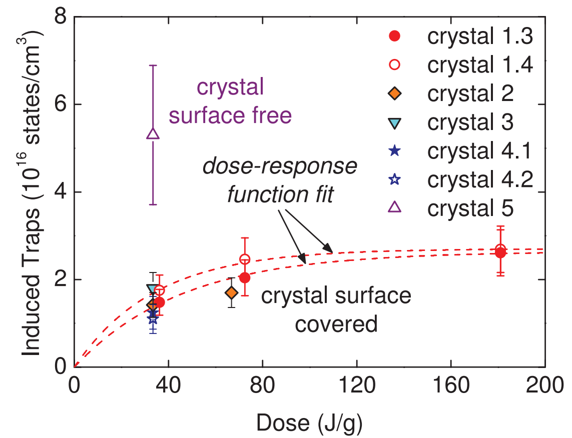

FIG. 6. (Color online) Induced trap density as a function of absorbed radiation dose. With increasing dose, the trap density rises sublinearly and saturates at high dose. The dose-response function given in Eq. (2) is fitted to the data points of crystal 1.3 and crystal 1.4 (dashed lines). Crystal 5 was irradiated after the top contact had been peeled off, resulting in a roughly three to five times higher trap density compared to crystals irradiated with the surface covered by the PDMS/Cr/Au top electrode.

energetically sharp level, which in turn may be slightly shifted in energy due to variations of the local environment and thus leads to an overall broader DOS peak. The main conclusion from this quantitative agreement (see also Fig. 2 of Ref. 8) is that the dose is the main parameter determining the density of induced traps.

Insight into the microscopic mechanisms can be gained from measuring the trap density for different radiation levels, that is, the dose-response curve. Therefore, two crystals were exposed stepwise to higher dose up to 180 J/g. Surprisingly, the density of additional traps increases sublinearly and saturates at high dose, as shown in Fig. 6. Such a curve can be approximated by a dose-response function of the form[17]

$$C = C_\infty(1 - e^{-Dk}), \tag{2}$$

where C is the trap density, C_∞ is the trap density at infinite dose, D is the dose, and k is a constant (dashed lines in Fig. 6). Saturation of the dose-trap density curve at such a low level of damage (∼1 trap per 50 000 molecules) reflects the interplay between trap generation and trap healing. We attribute the generation process to breaking-off a hydrogen from the rubrene molecule (which is possibly accompanied by lattice distortions and other defects). Detachment of hydrogen in organic compounds by high-energy irradiation is a known phenomenon[18–20] and is attributed to relatively weak bonding of the H atom to the C network.[21] Trap healing can take place if a hydrogen atom reattaches to a molecule where hydrogen has been previously removed. At high dose, both processes are in equilibrium.

Other than reattaching to a rubrene molecule with a missing H atom, some freed hydrogen may also desorb from the crystal. This scenario is possible if hydrogen diffuses through the crystal without being trapped and if the crystal surface is not covered. Encapsulation reduces desorption and increases the probability of H reattachment near the surface.[22,23] If this is the dominating microscopic process, the trap density is

expected to be higher for a given dose, when the crystal surface is free during irradiation. We have checked this hypothesis by carefully peeling off the PDMS/Cr/Au electrode before irradiation and relaminated it afterward for the TD-SCLC measurement. The result of this experiment fully confirms the proposed mechanism (purple △ in Fig. 6). For a proton dose of 35 J/g, the trap density is three to five times higher than in any crystal where the PDMS/Cr/Au electrode had not been removed for irradiation. Importantly, the DOS of the shielded reference remained unchanged within the measurement accuracy, which indicates that removing and reapplying the top contact produces no significant number of traps.

IV. CONCLUSIONS

To summarize, we quantitatively determined the creation of trap states in the bulk of rubrene single crystals upon proton and helium ion irradiation by TD-SCLC measurements. Our results show that with increasing radiation dose the trap density increases sublinearly in a well-defined energy range peaking at about 0.35 eV above the VB edge. At high radiation dose, trap creation, due to C–H bond breaking, is in equilibrium with trap healing due to reattaching H atoms, leading to a saturating trap density. Thus we have experimentally established the link between an electronic trap level and the underlying physical defect. Further insight could be gained by electronic structure calculations to delineate the contribution of only removing the H atom from the rubrene molecule, and the electronic level shift due to local distortion of the lattice.

ACKNOWLEDGMENTS

We gratefully acknowledge Jonathan Hanselmann, Roger Häusermann, Thomas Mathis, and Tobias Morf for support in the early stages of this study and for fruitful discussions.

*tino.zimmerling@phys.ethz.ch

[1] R. Friend, Mater. Sci. Forum **608**, 159 (2009).
[2] C. D. Dimitrakopoulos and P. R. L. Malenfant, Adv. Mater. **14**, 99 (2002).
[3] W. L. Kalb, S. Haas, C. Krellner, T. Mathis, and B. Batlogg, Phys. Rev. B **81**, 155315 (2010).
[4] W. L. Kalb and B. Batlogg, Phys. Rev. B **81**, 035327 (2010).
[5] R. W. I. de Boer, M. E. Gershenson, A. F. Morpurgo, and V. Podzorov, Phys. Status Solidi A **201**, 1302 (2004).
[6] V. Podzorov, E. Menard, A. Borissov, V. Kiryukhin, J. A. Rogers, and M. E. Gershenson, Phys. Rev. Lett. **93**, 086602 (2004).
[7] R. A. Laudise, C. Kloc, P. G. Simpkins, and T. Siegrist, J. Cryst. Growth **187**, 449 (1998).
[8] See Supplemental Material at http://link.aps.org/supplemental/10.1103/PhysRevB.85.134101 for details on the PDMS top contact preparation, TD-SCLC measurements using a PDMS top contact, and additional irradiation results.
[9] C. Krellner, S. Haas, C. Goldmann, K. P. Pernstich, D. J. Gundlach, and B. Batlogg, Phys. Rev. B **75**, 245115 (2007).
[10] F. Schauer, S. Nešpůrek, and H. Valerián, J. Appl. Phys. **80**, 880 (1996).
[11] S. Nešpůrek, O. Zmeškal, and F. Schauer, Phys. Status Solidi A **85**, 619 (1984).
[12] D. L. Bätzner, A. Romeo, M. Döbeli, H. Zogg, and A. N. Tiwari, Seventeenth European Photovoltaic Solar Energy Conference, Vol. II, OA9.3 (2001).
[13] J. R. Schwank, M. R. Shaneyfelt, and P. E. Dodd, *Radiation Hardness Assurance Testing of Microelectronic Devices and Integrated Circuits: Radiation Environments, Physical Mechanisms, and Foundations for Hardness Assurance,* Sandia National Laboratories (Sandia National Laboratories, Livermore, CA, 2008).
[14] J. Dacuña and A. Salleo, Phys. Rev. B **84**, 195209 (2011).
[15] J. F. Barbot, E. Ntsoenzok, C. Blanchard, J. Vernois, and D. B. Isabelle, Nucl. Instrum. Methods Phys. Res. B **95**, 213 (1995).
[16] J. F. Ziegler, J. P. Biersack, and U. Littmark, *The Stopping and Range of Ions in Solids*, 2nd ed., edited by J. F. Ziegler, Vol. 1 (Pergamon Press, New York, 1985).
[17] W. Snipes and P. K. Horan, J. Radiat. Res. **30**, 307 (1967).
[18] *Handbook of Modern Ion Beam Materials Analysis*, 2nd ed., edited by Y. Wang and M. Nastasi (Materials Research Society, Warrendale, PA, 2009).
[19] M. P. de Jong, A. J. H. Maas, L. J. van Ijzendoorn, S. S. Klein, and M. J. A. de Voigt, J. Appl. Phys. **82**, 1058 (1997).
[20] T. A. Tombrello, Nucl. Instrum. Methods Phys. Res. B **24**, 517 (1987).
[21] L. Torrisi, Radiat. Eff. Defects Solids **143**, 19 (1997).
[22] J. R. Fryer and F. M. Holland, Ultramicroscopy **11**, 67 (1983).
[23] J. R. Fryer, C. McNee, and F. M. Holland, Ultramicroscopy **14**, 357 (1984).